Bulletin of the Seismological Society of America, Vol. 97, No. 3, pp. 671–690, June 2007, doi: 10.1785/0120050150

An Overview of the Damaging and Low Magnitude M_w 4.8 La Paca Earthquake on 29 January 2005: Context, Seismotectonics, and Seismic Risk Implications for Southeast Spain

by B. Benito, R. Capote, P. Murphy, J. M. Gaspar-Escribano, J. J. Martínez-Díaz, M. Tsige, D. Stich, J. García-Mayordomo, M. J. García Rodríguez, M. E. Jiménez, J. M. Insua-Arévalo, J. A. Álvarez-Gómez, and C. Canora

Abstract This article presents an overview of the La Paca earthquake of magnitude m_{bLg} 4.7, which occurred on 29 January 2005, with its epicenter located near the town of Avilés in the Murcia region in southeast Spain. Despite its low magnitude, the earthquake caused important damage in two towns of the epicentral area, La Paca and Zarcilla de Ramos. These areas recorded intensities of VI–VII (European Macroseismic Scale, 1998) and sustained estimated economic losses amounting to 10 million €. Aftershocks continued for more than 2 weeks, producing considerable alarm in the population and mobilizing emergency services from the whole region. The La Paca seismic series is the third registered in the region in the past 8 years, being preceded by the Mula (1999) and southwest Bullas (2002) seismic series. These main events had also low magnitudes (m_{bLg} 4.8) and caused damage levels similar to the 2005 earthquake. The case is an example of a moderate seismic zone where low-magnitude and frequent earthquakes have important implications on the seismic hazard and risk of the region. Although these are not the largest expected earthquakes, they have yielded important information for improving the knowledge of the seismic activity of the area. With this aim in mind, different topics have been analyzed from a multidisciplinary perspective, including seismicity, local tectonics and surface geology, focal mechanisms, macroseismic effects, and ground motion. Results indicate a local tectonic interpretation, consistent with a strike-slip focal mechanism, the confirmation of a triggering process between the 2002 and 2005 earthquakes, a geotechnical and ground-motion characterization for the damaged sites (supporting local amplification effects and estimated peak ground acceleration values of $\sim 0.1g$), and an understanding of damage patterns in relation to local building trends. The results may be used as guidelines for future revisions of the Spanish Building Code (Norma de la Construcción Sismorresistente Española [NCSE-02], 2002). The study results should contribute to risk mitigation in a region where strong-motion records from the maximum expected earthquakes are not available. This approach can be extended to other regions with similar seismic backgrounds and a lack of strong-motion records.

Introduction

The 2005 series began on the 29 January, when an earthquake of magnitude m_{bLg} 4.7 or M_w 4.8 took place near the town of Avilés (Murcia region, southeast Spain). This is the third earthquake resulting in considerable damage in the Murcia region in the past 8 years, following the earthquakes of Mula (2 February 1999, m_{bLg} 4.8) and southwest Bullas (6 August 2002, m_{bLg} 4.8). The three earthquakes reached intensities of VI–VII (European Macroseismic Scale 1998 [EMS-98]), causing important economic losses but fortunately no casualties. We refer to this earthquake as the 2005 La Paca earthquake in allusion to one of the most damaged towns.

The Murcia region is an area with moderate seismic activity in Spain, with a regional stress field related to the convergence of the African and Eurasian plates. In this area, relatively frequent earthquakes with low-to-moderate mag-

nitudes take place, having caused damage in historical and recent times. Temporal clustering of significant events has eventually been identified in the region. Since 1999, three damaging earthquakes have occurred in a short time. This timing raises the possibility of a triggering mechanism that may initiate further events in the near future, provoking corresponding concerns for the regional seismic risk and hazard status.

The heaviest damage in the 2005 earthquake was not observed in the town nearest to the epicenter (Avilés), but in other more distant locations (La Paca and Zarcilla de Ramos), where first assessments established macroseismic intensities of VI and VII (EMS-98), respectively. Several factors influencing the damage distribution are analyzed: site conditions, input ground motion, and the vulnerability of local construction trends.

Ground-motion values of up to 0.024*g* were obtained for the 2005 series at strong-motion stations located more than 20 km from the epicenter of the main event. No strong-motion records are available in the epicentral area for direct characterization of the ground motion in that location. This same problem was encountered for the 1999 and 2002 earthquakes. For this reason, the simulation of the ground motion is of particular interest for inferring strong-motion and response spectra values for both the epicentral area and the locations of the most damaged towns of La Paca and Zarcilla de Ramos. In these locations damage was reported to modern code-compliant engineered structures. This is a critical point regarding revisions of the building code and future risk mitigation in the region.

This article presents an overview of the conclusions resulting from a multidisciplinary analysis of this striking case, incorporating geological, seismological, and architectural data. The purpose is twofold: (1) to gather as much information as possible regarding the earthquake's characteristics and effects, such as the spatial and chronological distribution of events, focal parameters of significant shocks, strong-motion records, and damage reports, and (2) to infer from these data explanations for the unexpected damage distribution, evidence relating this event back to the 2002 southwest Bullas event, and possible implications for the regional seismic-hazard levels. Achieving this purpose requires the analysis of local-scale fault kinematics, local soil conditions, and local building practices.

Seismic Hazard and Regional Seismotectonic Framework for the Murcia Region

Seismic Hazard

The epicenter of the 2005 La Paca earthquake, as well as those of the previous series of 1999 and 2002, is located in the southwest of the province of Murcia, a zone with moderate seismic hazard. A first view of the relative hazard for this zone compared with other regions in Spain is obtained from the hazard map of the Spanish earthquake-resistant building Code NCSE-02 (Norma de la Construcción Sismorresistente Española [NCSE-02], 2002), shown in Figure 1. The represented value is the NCSE-02 basic acceleration, a_b, corresponding to horizontal peak ground acceleration (PGA) in hard soil with a 10% probability of being exceeded in 50 years. Expected a_b values for the Murcia region range between 0.04 and 0.16*g*. Alongside Granada and Alicante, Murcia is one of the regions with the highest hazard levels in Spain.

Regional Tectonic Setting

The study area is located in the external zone of the Southeastern Betic Cordilleras (Fig. 2a). The epicentral region is characterized by a complex tectonic structure due to its position between a major shear zone, the Crevillente Fault Zone, also known as the Cádiz-Alicante Fault (Sanz de Galdeano 1983), and the contact between the Internal and External zones (Hermes 1978, 1985). The Crevillente fault is a 150-km-long dextral strike-slip fault, active during the late Miocene and early Tortonian (Martínez-Díaz, 1998; Sanz de Galdeano and Buforn, 2005). Strike-slip motion along the fault has contributed to the westward emplacement of the Alborán Domain units of the internal zones (Andrieux *et al.*, 1971; Sanz de Galdeano, 1990). These movements produced a regional morphostructure characterized by northeast–southwest-trending ranges of Jurassic limestones separated by Triassic gypsums and Cretaceous-Tertiary marls.

Since the Late Miocene, the Crevillente fault has been unfavorably aligned for strike-slip motion because its N70°E trend is normal to the current regional shortening direction (Sanz de Galdeano and Buforn, 2005). During the Upper Miocene-Pliocene, marine basins were developed to the north of the Crevillente fault, while to the south, Pliocene lakes filled the depressions between the Sierras. N50°E strike-slip left-lateral faults, coherent with the current stress field, have been created or reactivated in the region since the Tortonian onward, affecting the Pliocene and the Pleistocene deposits. Paleoseismic studies on some of these faults (i.e., the Alhama de Murcia Fault; Fig. 2b) report a significant palaeoseimic activity during the Holocene and several surface ruptures have been identified (Martínez Díaz *et al.*, 2001).

Historical and Instrumental Seismicity in the Region

The historical seismicity reported for the Murcia region includes several damaging earthquakes. The location and intensity of these earthquakes, with estimated intensities I ≥ VII are given in Table 1. Epicenters are shown in Figure 3.

The first earthquake of which we have knowledge occurred in 1579, with intensity VII. Another earthquake reached intensity VIII in 1674, and two additional earthquakes are reported in 1911 with the same intensity, causing significant damage in Torres de Cotillas and Lorquí. These earthquakes have been the subject of several reports:

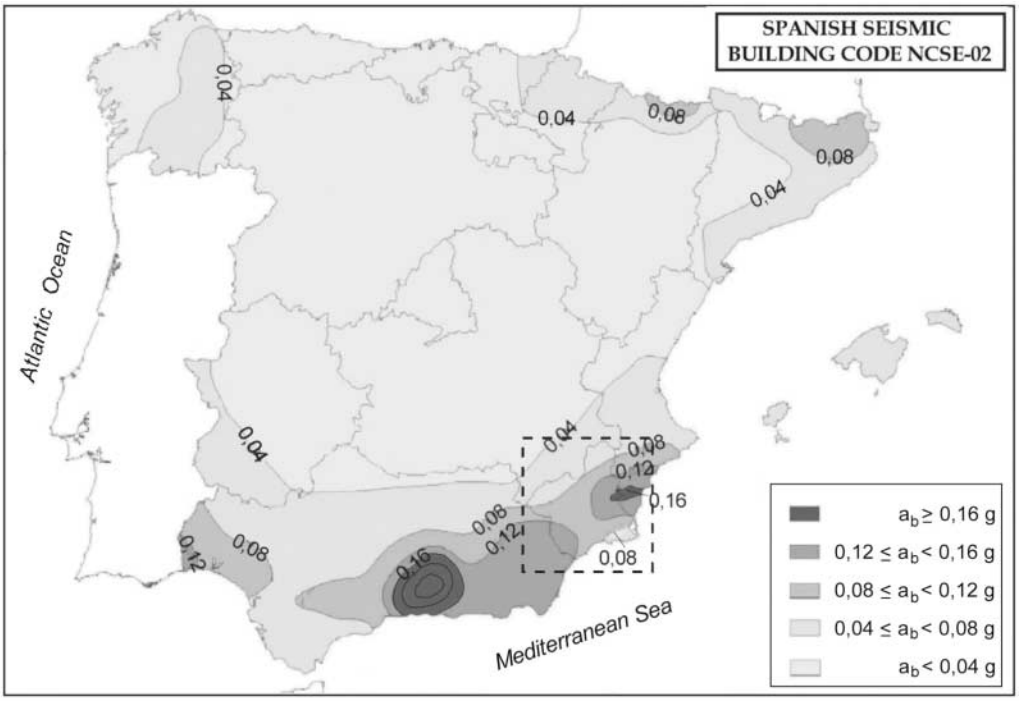

Figure 1. Seismic-hazard map of the Spanish Building Code NCSE-02. Isolines represent "basic acceleration, a_b," which corresponds to the expected PGA in hard soil for exceedence probabilities of 10% in 50 years. The Murcia province is framed with a rectangle.

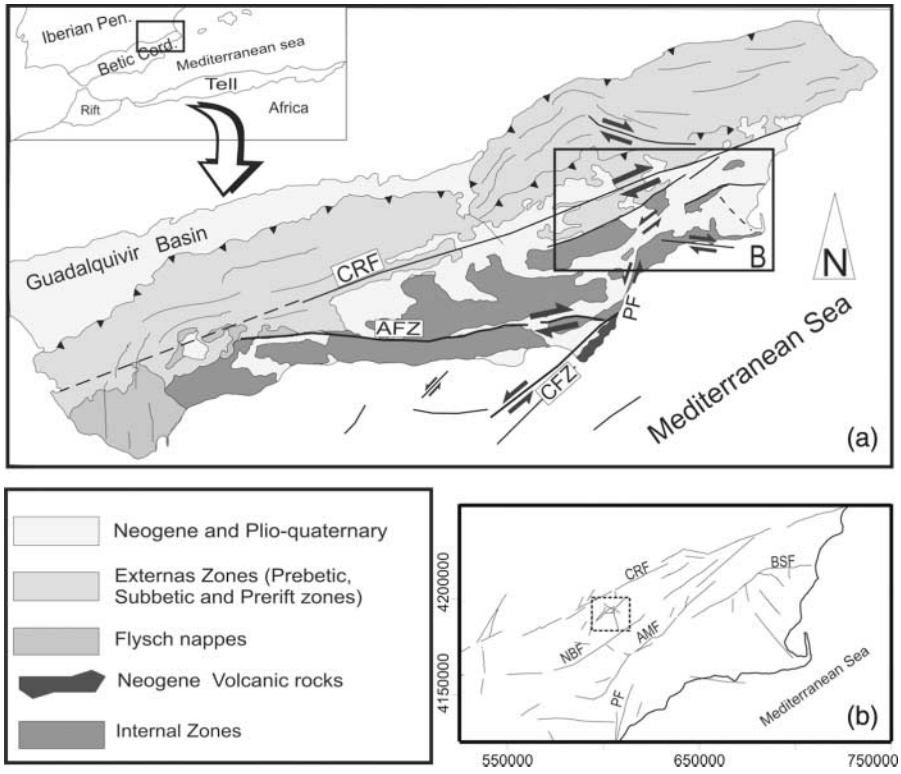

Figure 2. (a) Geological map of the Betic Cordillera and surrounding areas. The rectangle shows the location of the studied area. CRF, Crevillente fault; AFZ, Alpujarras fault zone; CFZ, Carboneras fault zone; PF, Palomares fault. (Modified from Martínez-Díaz, 1998.) (b) Principal faults with Quaternary activity identified in the area around the epicenter of the 2005 Bullas sequence. CRF, Crevillente fault; AMF, Alhama de Murcia fault; PF, Palomares fault; BSF, Bajo Segura fault. (Modified from Martínez-Díaz, 1998.)

Table 1

Location Data, Epicentral Intensity (I_0, EMS) and Magnitude (m_{bLg}) of the Earthquakes That Have Occurred in Murcia Province with $I_0 >$ VII and/or $m_{bLg} \geq 4.0$

Date (yyyy/mm/dd)	Time UTC (h:m:s)	Longitude (° W)	Latitude (° N)	Depth (km)	Location	Maximum Intensity (EMS)	Magnitude m_{bLg}
1579/01/30	?	1.70	37.68		Lorca	VII	
1674/08/28	21:30:00	1.70	37.68		Lorca	VIII	
1743/03/09	16:00:00	1.13	38.00		Murcia	VII	
1907/04/16	17:30:00	1.50	37.80		Totana	VII	
1908/09/29	00:00:00	1.30	38.10		Ojós	VII	
1911/03/21	14:15:35	1.21	38.01		Torres de Cotillas	VIII	
1911/04/03	11:11:11	1.20	38.10		Lorquí	VIII	
1917/01/28	22:32:31	1.26	38.03		Torres de Cotillas	VII	
1930/09/03	09:59:58	1.23	38.06		Lorquí	VII	
1944/02/23	22:34:10	1.15	38.16		Fortuna	VII	
1948/06/23	03:43:55	1.75	38.14		Cehegín	VIII	
1972/04/14	03:22:17	1.35	38.47	5	Jumilla		4.2
1977/06/06	10:49:12	1.73	37.64	9	Lorca	VI	4.2
1978/03/24	13:01:24	1.70	37.63	5	Lorca		4.3
1995/11/26	05:39:40	1.27	38.03	2	N. Alcantarilla	V–VI	4.1
1996/09/02	19:07:01	1.55	37.56	1	Mazarrón	V	4.5
1999/02/02	13:45:18	1.50	38.09	1	Mula	VI	4.8
2002/08/06	06:16:19	1.83	37.88	1	Southwest Bullas	VI*	4.8
2005/01/29	07:41:31	1.78	37.88	3	La Paca	VII*	4.7

Data extracted from the IGN database (Mézcua and Martínez Solares, 1983; Martínez Solares and Mézcua, 2002; and the IGN website, www.ign.es) except (*), which are our own data.

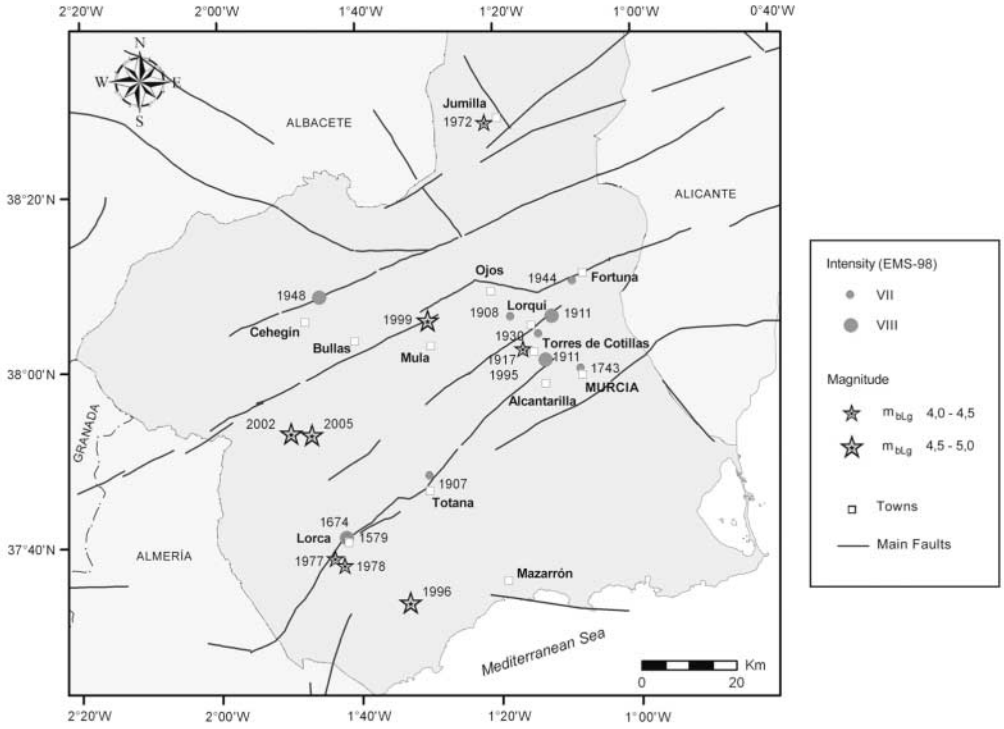

Figure 3. Epicenters of the major earthquakes that have occurred in Murcia Province ($I_0 >$ VII and/or $m_{bLg} \geq 4.0$). Location parameters are given in Table 1.

Jiménez Cisneros (1911), Sánchez Lozano and Marín (1912), Sánchez Navarro-Neumann (1911, 1912, 1917, 1920), Galbis (1932), and Rey Pastor (1936). The magnitudes were estimated as M_s 5.7 ± 0.5 and 5.3 ± 0.3 for the March and April 1911 events, respectively (Buforn *et al.*, 2005).

After the 1911 series, no sizable earthquakes occurred in the Murcia region, until an event on 23 June 1948, located 60 km to the west of the 1911 series (Fig. 3). According to Rey Pastor (1949), the maximum intensity of the 1948 event was VIII Forell–Mercalli and its magnitude was 5.3 (Badal *et al.*, 2000).

The seismic activity of the area has continued during the period of instrumental records. Table 1 includes the data of all the earthquakes from 1972 onward with magnitude greater than or equal to 4.0. The epicenters of these earthquakes are shown in Figure 3 together with the epicenters of historical earthquakes.

Between the last historical event of 1948 and 1996, five earthquakes took place with magnitudes between 4.0 and 4.5 (m_{bLg}). On 2 February 1999, an earthquake with m_{bLg} 4.8 occurred near the town of Mula (Fig. 3), starting a period of higher activity in the region. A maximum intensity of VI (EMS) was observed in Mula, Torres de Cotillas, Campos del Río, and other towns along the Mula river. This earthquake was felt at far distances, such as Madrid (400 km). This event was preceded by a foreshock and followed by numerous aftershocks, two of them with magnitudes greater than 3.5. The mainshock has been the subject of several studies (Instituto Geográfico National [IGN], 1999; Buforn and Sanz de Galdeano, 2001; Martínez-Díaz *et al*., 2002; Mancilla *et al.*, 2002).

Another earthquake with m_{bLg} 4.8 (IGN) occurred on 6 August 2002 near the town of Bullas, 20 km west of Mula. The so-called southwest Bullas earthquake reached a maximum EMS intensity of VI in Bullas and Cehegín and was also followed by numerous aftershocks, three of them exceeding magnitude 3.5.

Based on the analysis of historical and instrumental events, we observe an activity pattern composed of a cluster of moderate magnitude events ($M \approx 5$) lasting a few years, separated by longer periods of quiescence. This pattern can be observed between the years of 1907 and 1917 and the 1940s, with maximum intensities of I = VIII (see Table 1).

Local Seismotectonic Setting for the La Paca (2005) Earthquake

In this section we analyze the geographical and chronological distribution of the 2005 seismic series in terms of the tectonic setting of the epicentral area. The 1999 and 2002 series are also analyzed here because of their relevance to the 2005 series on account of their geographical and chronological closeness.

Seismic Description of the 2005 Series: Spatial and Chronological Distribution

The La Paca earthquake was located near the town of Avilés (Fig. 4). This shock was followed by an important aftershock series lasting more than 2 weeks. The epicenters of the seismic series are shown in Figure 4, together with epicenters of the previous series of 1999 and 2002 (locations given by IGN). As we can see from the figure, the epicenters of the 2002 and 2005 series partly overlap each other.

The epicenters of the events following the mainshock between 29 January and 7 February are represented in 2-day intervals in Figure 5. Analysis of these events suggests that the 29 January shock triggered an aftershock sequence with a north–south to northeast–southwest trend. The activity started to decrease after 31 January. On 3 February a new event with magnitude 4.2 (m_{bLg}) took place, triggering another aftershock series, extending predominately northward from the epicenter. The aftershock activity was thereby reactivated by this event. Figure 6a shows a representation of the number of events per day. The number of events clearly decreased during the 2 days after the mainshock of 29 January, rising again after the 3 February event. The whole process seems to indicate that the two ruptures took place on different faults or fault segments.

We can support this hypothesis by comparing the decay of aftershock activity with the common exponential pattern proposed by Omori (1884), which in logarithmic form corresponds to the expression: $\log N(t) = a - b \cdot \log t$, with $N(t)$ being the number of events per day and t the time (in days) elapsed after the mainshock. A fit to the complete series yields a poor correlation coefficient, whereas independent fits for both seismic subseries confirm that these adjust better to Omori's law. Figure 6b (left and right) shows the fit for the two subseries.

Finally, we have studied the magnitude–frequency distribution of the aftershocks, comparing it with the common power law of the Gutenberg–Richter relation ($\log N(m) = a - b\,m$, where m is the magnitude and $N(m)$ is the cumulative number of earthquakes with magnitude $M \geq m$). We found a value of $a = 2.71$, $b = 0.64$ for the first, and $a = 3.56$, $b = 0.90$ for the second subseries. Large correlation coefficients of $R^2 = 0.96$ and $R^2 = 0.99$, respectively, indicate that both subseries follow closely a magnitude–frequency distribution consistent with the Gutenberg–Richter law.

Focal Mechanism

The 2005 La Paca earthquake sequence was recorded at a dense regional network of broadband seismographs. We use waveforms from 12 near-regional stations to estimate moment-tensor mechanisms and magnitudes for the La Paca mainshock and major aftershocks. We represent seismic waveforms as a linear combination of 1D Greens' functions for an average, regional velocity, and density model (Stich

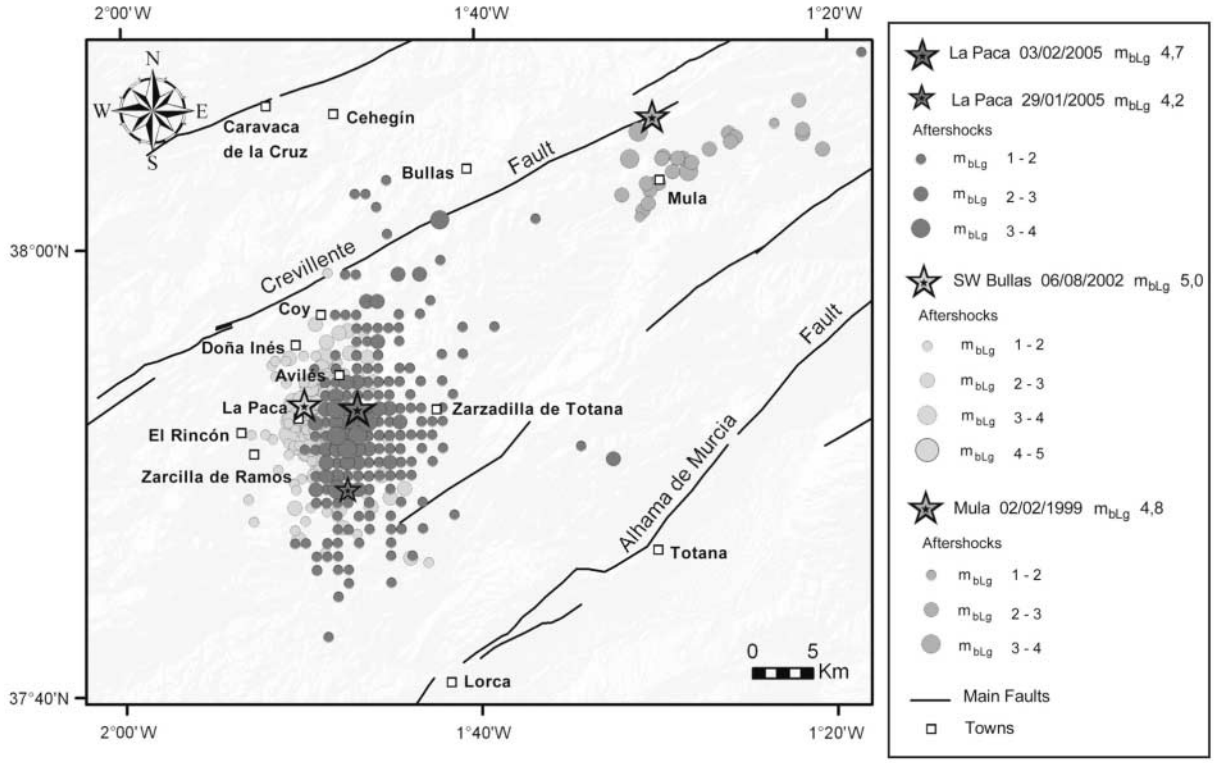

Figure 4. Epicenters of the mainshocks and aftershocks for the 1999 Mula, 2002 Bullas, and 2005 La Paca series. Main faults are also shown in the map.

et al., 2005), and invert for the deviatoric moment tensor by minimizing the L2-misfit between observed and predicted time-domain displacement seismograms (Langston *et al.*, 1982). Waveforms are filtered in an intermediate period band (20–50 sec for the mainshock) to obtain appropriate path corrections. A more detailed discussion of the inversion scheme is given in Stich *et al.* (2003).

Moment-tensor inversion for the 2005 La Paca mainshock yields a seismic moment of $1.6 \cdot 10^{16}$ N m and a moment magnitude M_w 4.8. The best moment tensor corresponds to a nearly double-couple force system (3% non-double-couple reminder [CLVD]), showing predominately strike-slip movement with a minor normal component (Tables 2 and 3). Our result is similar to an automatic near-real-time moment-tensor estimate by IGN-Madrid (www.ign.es). The right-lateral nodal plane has strike N132°E, dip 85°, and rake $-153°$, the left-lateral nodal plane has strike N40°E, dip 63°, and rake $-5°$. This solution corresponds to generally good waveform matches, except for unmodeled near-field contributions (Fig. 7).

In the same way, we obtain stable inversion results and adequate waveform matches for three events of the La Paca aftershock sequence, with moment magnitudes between 3.6 and 4.2 (Table 2). For all events, we have estimated the upper crustal source depths. Moment-tensor mechanisms differ noticeably from the mainshock mechanism, supported by the corresponding differences in intermediate period waveforms (Fig. 7). The aftershock mechanisms show larger normal components than the mainshock, specifically rather steep ~east-southeast–west-northwest striking right-lateral nodal planes, and quite shallow ~north–south striking left-lateral nodal planes. This suggests considerable geometric complexity and an off-fault origin for these aftershocks. This result agrees with the hypothesis of two possible ruptures, as deduced from the temporal pattern of aftershock activity (see "Seismic Description of 2005"). The earthquakes of 3 and 4 February show nearly identical broadband waveforms and can be considered a duplet indicating repeated rupture of the same fault patch (Geller and Mueller, 1980). This is consistent with our nearly identical moment-tensor mechanisms for these events.

For the 1999 and 2002 sequences, several focal mechanisms have been given by routine moment tensor projects at Istituto Nazionale di Geofisica e Vulcanologia (INGV), Italy (Pondrelli *et al.*, 2002), ETH Zürich, Switzerland (Braunmiller *et al.*, 2002), and Instituto Andaluz de Geofísica (IAG)-Granada, Spain (Stich *et al.*, 2003), as well as in individual studies. For the 2002 series, we reprocessed moment-tensor estimates from the IAG catalog, including further near-regional recordings from the temporary TEDESE network (ROA/UCM/Geofon). Moment-tensor solutions for the mainshock (M_w 5.0) and three aftershocks (M_w 3.5–4.0, www.ugr.es/~iag/tensor) show oblique normal faulting, with ~north–south (N0°E to N11°E) and ~west-northwest–

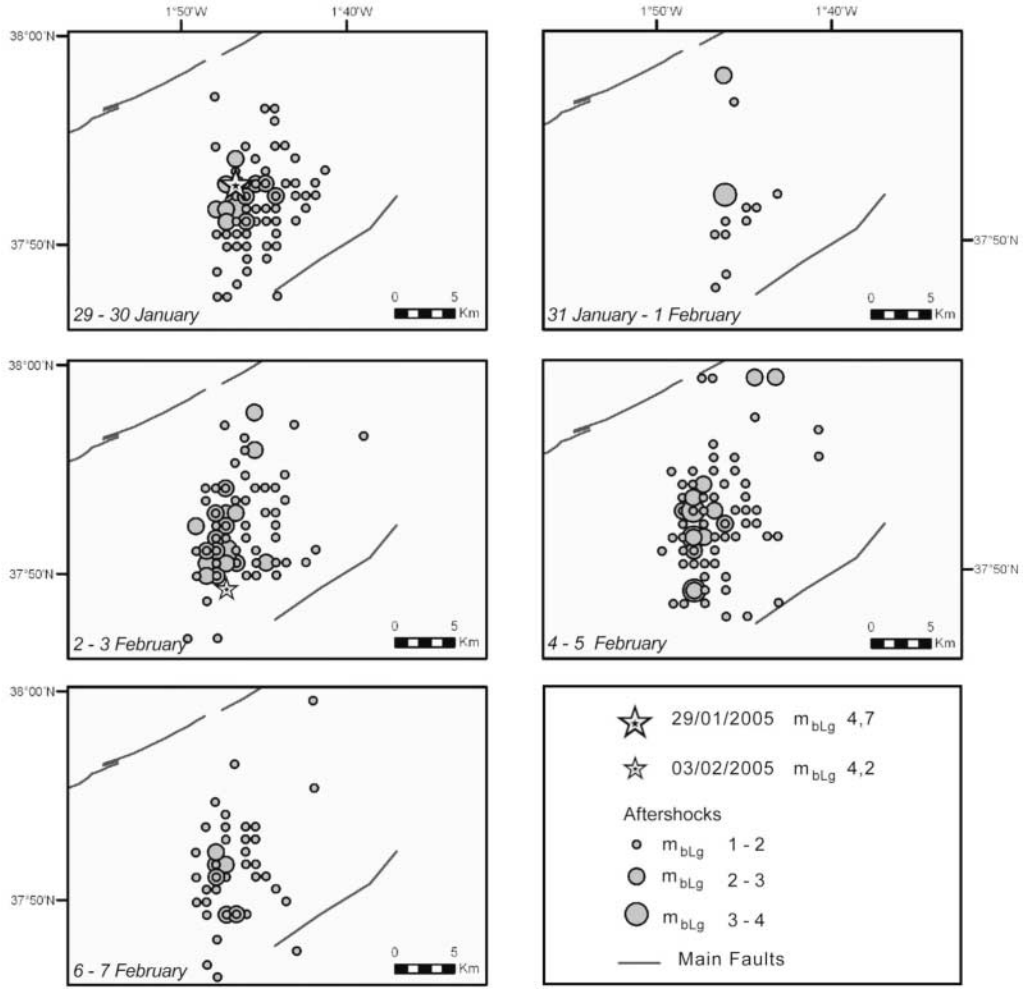

Figure 5. Space–time distribution of epicenters of the 2005 seismic series. The epicenters of the aftershocks are shown in time windows of 2-day duration.

east-southeast (N115°E to N130°E) striking nodal planes, very similar to the M_w 3.6 aftershock of 1 February 2005.

For the 1999 Mula earthquake, two similar moment-tensor estimates are available from full-waveform inversion at seven and eight near-regional stations, respectively (Mancilla *et al.*, 2002; Stich *et al.*, 2003), indicating magnitude M_w 4.7–4.8, and predominately strike-slip faulting, very similar to the 2005 La Paca mainshock. In contrast, the focal mechanism from first motion polarities (Buforn and Sanz de Galdeano, 2001) indicates predominately reverse faulting, in good agreement with the INGV moment tensor from the long-period, sparse network data. We prefer the strike-slip solution (Table 2), because the first-motion polarity pattern is equally consistent with both a strike-slip and a reverse solution (Buforn *et al.*, 2005), and the incorporation of intermediate-period surface wave observations from the Spanish network clarifies this ambiguity (in this case increasing L2 misfit by a factor of 2 for the reverse solution; see Mancilla *et al.*, 2002).

Local Tectonic Setting

Structure in the Epicentral Area. To correlate the recent seismic activity in the La Paca area with the main tectonic structures in the region, we have carried out a geological field survey and a review of the existing geological 1:50,000 scale maps (Kampshuur *et al.*, 1972a,b; Jerez Mir *et al.*, 1974; Velando and Paquet, 1974). This study was complemented with the analysis of field evidence for possible Quaternary deformation with the aim of characterizing the possible source of the earthquakes. We found several high-angle brittle postalpine or neotectonic faults (Fig. 8), which are good candidates for the source of the La Paca seismic series. The main characteristics of these faults are summarized in Table 4. Most of these faults show a curved geometry in the epicentral area (Avilés-La Paca-Zarcilla de Ramos), indicating bending of the mainfault traces.

The most relevant fault group is in a zone that crosses the epicentral area from northeast to southwest and probably

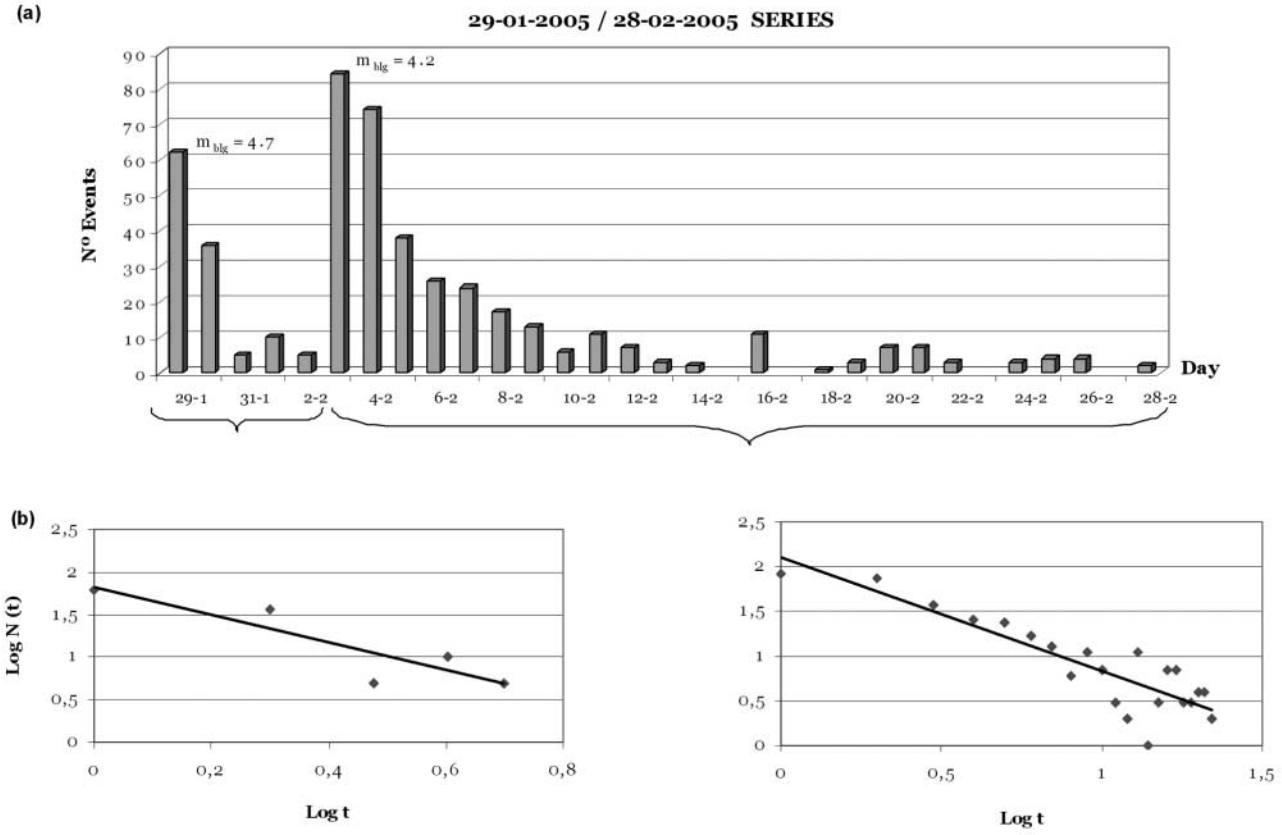

Figure 6. (a) Number of events per day, from 29 January until 18 February 2005. Two different series may be observed. (b) Adjustment to the Omori law for the two seismic series: from 29 January until 2 February (left) and from 3 February until 28 February 2005 (right). The inferred parameters are $a = 1.82$, $b = 1.63$ for the first, and $a = 3.38$, $b = 2.08$ for the second subseries. The corresponding correlation coefficients are $R^2 = 0.80$ and $R^2 = 0.74$, respectively.

Table 2

Location Parameters, Magnitude, and Moment Tensor Solutions for the 2005 La Paca and the 2002 Bullas Sequence (This Study), and the 1999 Mula Mainshock (Stich *et al.*, 2003)

Date (yyyy/mm/dd)	Time	Latitude (°)	Longitude (°)	Depth (km)	Fault-Angle Parameters (Strike/Dip/Rake)	CLVD (%)	M_0 (N m)	M_w
1999/02/02	13:45:17	38.11	−1.49	6	141/66/−157; 41/69/−25	8	$1.65\cdot10^{16}$	4.8
2002/08/06	06:16:19	37.91	−1.82	8	119/68/−140; 11/53/−27	3	$3.47\cdot10^{16}$	5.0
2002/08/06	11:55:16	37.89	−1.81	6	115/73/−122; 0/35/−28	15	$8.81\cdot10^{14}$	3.9
2002/08/07	00:43:56	37.86	−1.83	6	120/74/−124; 7/37/−27	13	$2.34\cdot10^{14}$	3.5
2002/08/07	23:09:07	37.86	−1.84	6	130/70/−122; 11/37/−33	15	$1.08\cdot10^{15}$	4.0
2005/01/29	07:41:31	37.88	−1.78	10	132/85/−153; 40/63/−5	3	$1.62\cdot10^{16}$	4.8
2005/02/01	23:53:56	38.02	−1.70	6	120/68/−125; 1/40/−35	6	$2.61\cdot10^{14}$	3.6
2005/02/03	11:40:33	37.82	−1.79	10	110/84/−136; 15/46/−7	6	$2.44\cdot10^{15}$	4.2
2005/02/04	01:09:41	37.82	−1.80	6	109/82/−136; 11/47/−10	3	$8.65\cdot10^{14}$	3.9

Fault angle parameters for both nodal planes represent the double-couple component. The non-double-couple reminder (CLVD) of the moment tensor is given in percentage. M_0 is seismic moment and M_w is moment magnitude. Epicenter locations and origin times are taken from the IGN bulletin (IGN data file, www.ign.es).

continues out beyond the studied zone. The structures forming this system are the Avilés, Don Gonzalo, and Zarcilla faults (Fig. 8), all of them with left-lateral strike-slip activity and exhibiting similar branching and linkage patterns between fault sections. The Avilés and Don Gonzalo faults show a restraining stepover in the La Paca area with right-stepping and overlapping structural geometry. The 2.5-km overlap and 2-km separation among these faults produces high compressive deformation and tectonic stress concentration.

Table 3
Input Parameters for the Coulomb Stress Transfer Modeling for the 2002 and 2005 Mainshocks

Date (yyyy/mm/dd)	Fault-Plane Parameters (Strike/Dip/Rake)	Center of Rupture: Latitude (° N)	Center of Rupture: Longitude (° W)	M_w	Depth (km)	Rupture Area Length × Width (km × km)
2005/01/29	40/63/−5	37.88	1.78	4.8	5	2.4 × 2.4
2002/08/06 (Plane A)	11/53/−27	37.91	1.82	5.0	1	3 × 3
2002/08/06 (Plane B)	119/68/−140	37.91	1.82	5.0	1	3 × 3

Rupture area (width × length) is estimated using the equations of Wells and Coppersmith (1994). Note that for the 2002 event, two fault-plane solutions are considered.

Seismotectonic Interpretations for the 2005 Main Earthquake. Seismic data and field evidence allow us to identify the Avilés fault as the source of the main 29 January 2005 earthquake. The calculated focal mechanism solution indicates that the active fault responsible for this shock is a N45°E fault with strike-slip movement located near the town of Avilés. An alternative interpretation is that the same focal mechanism is produced by a dextral strike-slip fault trending northwest–southeast, which can be related with the El Puerto fault.

The geological and geomorphological field evidence collected in the area around the epicenter suggests that the Avilés fault is the most likely source of the 2005 mainshock. This fault was active during the Quaternary and recent geological times. Toward the southwest, at Umbría hill, the fault trace crosses and deforms a conglomerate continental formation dated as Plio-Quaternary according to geomorphological criteria. The conglomerates show a dense set of fractures aligned N80°E over the fault trace. These fractures are absent in other areas of the formation; we therefore conclude that this brittle deformation is evidence of fault movement occurring after the formation of these units.

The Local Tectonic Framework of 2002 Bullas Earthquake. The main Bullas earthquake on 6 August 2002 (M_w 5.0 or m_{bLg} 4.8) and its bigger aftershocks are located in an area about 2 to 3 km north of La Paca and away from the Avilés fault trace. The focal mechanisms indicate normal slip (with strike-slip component) on northwest–southeast-oriented faults. The El Puerto fault (Fig. 8), which crosses through the epicenter area, is a likely source candidate for the main earthquake of this series. Its orientation varies from N125°E to N100°E, similar to the orientation of the planes of focal mechanisms. The normal slip indicated by the focal mechanism results is in agreement with the northwest–southeast horizontal shortening direction.

Two theories may be proposed to explain why the series of 2002 and 2005 have occurred in the same region within a short time span. The first one would be a triggering process initiated after the 2002 series, caused by static stress transfer produced by the El Puerto fault motion. The other one would be related to the local tectonic configuration of the La Paca-Avilés area, where the restraining stepover between the Avilés and Zarcilla faults (Fig. 8) may produce continuous stress concentration in this relatively small area, promoting periodic slip events along different faults or fault segments.

Coulomb Failure Stress Modeling

Two seismic sequences in neighboring areas with significant material damage in the short time span of 3 years justifies looking into changes in the state of stress as a possible cause–effect process in operation. Such changes may advance or delay the failure of faults in the region, as proposed in other seismically active regions (Stein, 1999; Freed and Lin, 2001; Zeng, 2001; Pollitz, 2002).

It is known that the stress drop on a fault plane due to the occurrence of an earthquake increases the effective shear stress around the rupture area (Chinnery, 1963). During the past 10 years, observations from different seismic sources and their magnitudes have indicated that small variations in static stress, even lower than 1 bar, are able to induce the reactivation of nearby faults that are close to failure. This phenomenon has been described as a triggering process (Jaume and Sikes, 1992; King *et al.*, 1994; Harris *et al.*, 1995; Toda *et al.*, 1998). The triggering process may involve not only the generation of aftershocks or major shocks, but also changes of seismicity rate in a certain zone, increasing or decreasing for several months after a mainshock (Stein, 1999).

The triggering effect is attributed to changes in Coulomb failure stress (CFS): $\mathrm{CFS} = \tau_\beta - \mu\,(\sigma_\beta - p)$, where τ_β is the shear stress over the fault plane, σ_β is the normal stress, p is the fluid pressure, and μ is the frictional coefficient.

Following this approach, we have estimated the stress change produced by the 2002 and 2005 earthquakes by following the Okada (1992) method, taking a value of $3.2 \cdot 10^{10}$ N m^{-2} as the shear module and a value of 0.25 as Poisson's coefficient. The apparent friction coefficient is taken as 0.75, which is an acceptable value as proposed by several authors from the study of 10 years of activity in southern California (Toda and Stein, 2003). The orientation of the planes was selected from the moment-tensor mechanisms discussed previously (Table 3). The ruptures are modeled as rectangles with a rupture area estimated by using the equations of Wells and Coppersmith (1994). The parameters of the models are described in Table 3.

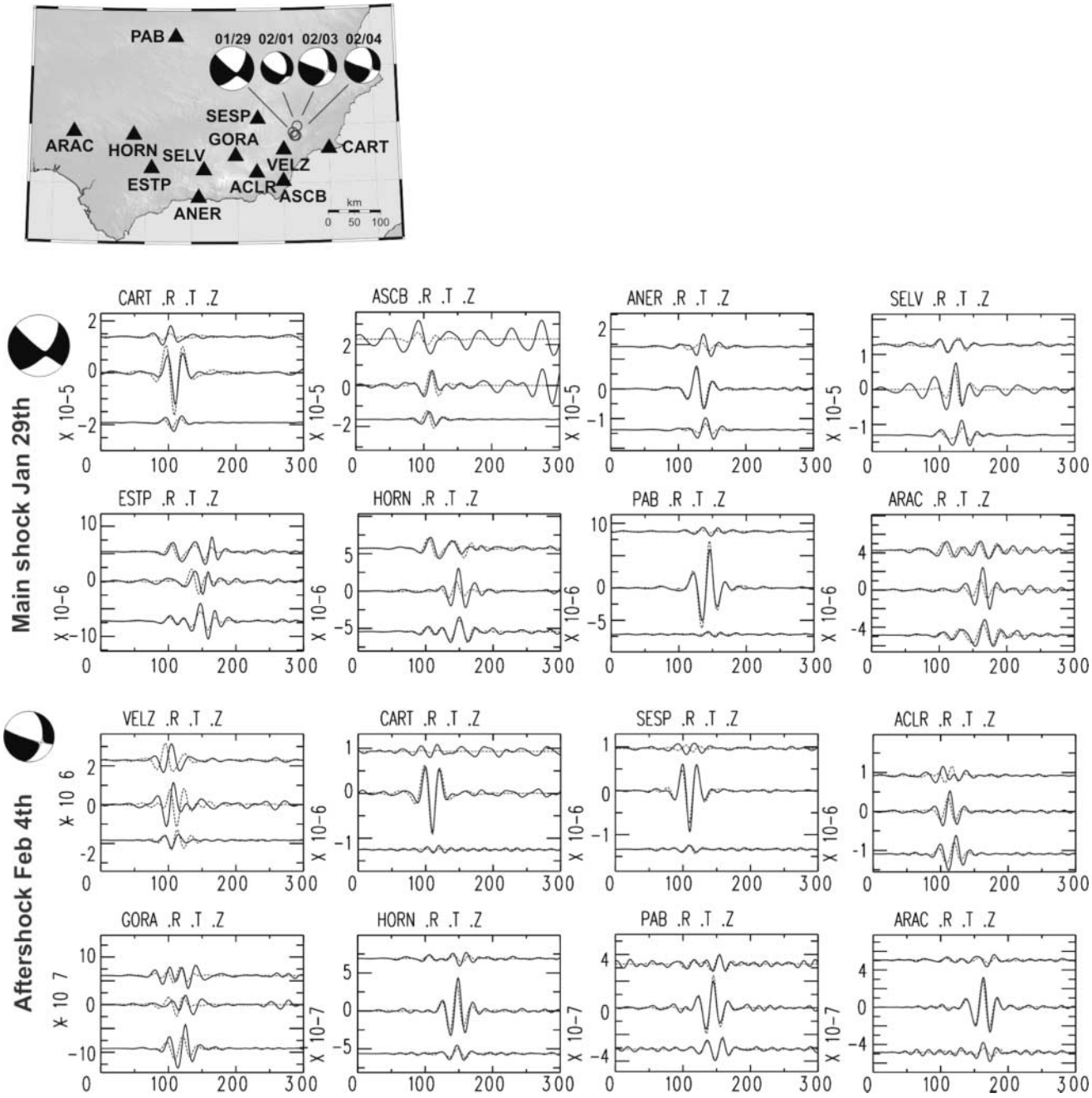

Figure 7. Sample waveform matches for moment-tensor solutions of the 2005 La Paca mainshock and the 4 February aftershock. Each waveform panel shows, from top to bottom, radial, transverse, and vertical intermediate period displacement waveforms (solid lines, observed seismograms; dotted lines, moment tensor predictions). The map shows the distribution of regional broadband stations used, and moment-tensor estimates for the mainshock and largest aftershocks (Tables 2 and 3). The remaining solutions are posted online at the IAG-Granada moment tensor project (www.ugr.es/~iag/tensor).

Figure 9 shows the stress transfer produced by the 2002 and 2005 mainshocks considering the two fault plane solutions for the 2002 mainshock. The stress changes produced by this event are calculated on planes parallel to planes oriented 40° N dipping 63° to the southeast, which is the source plane supported by geological data to be the responsible of the 2005 event (Fig. 9a, b). The stress change produced by the two mainshocks is calculated on optimally oriented planes for a strike-slip stress field with a maximum horizontal stress 169° N, in accordance with the present stress determinations of Stich *et al.* (2006) (Fig. 9c, d). These models show that the 2005 event occurred in an area where the

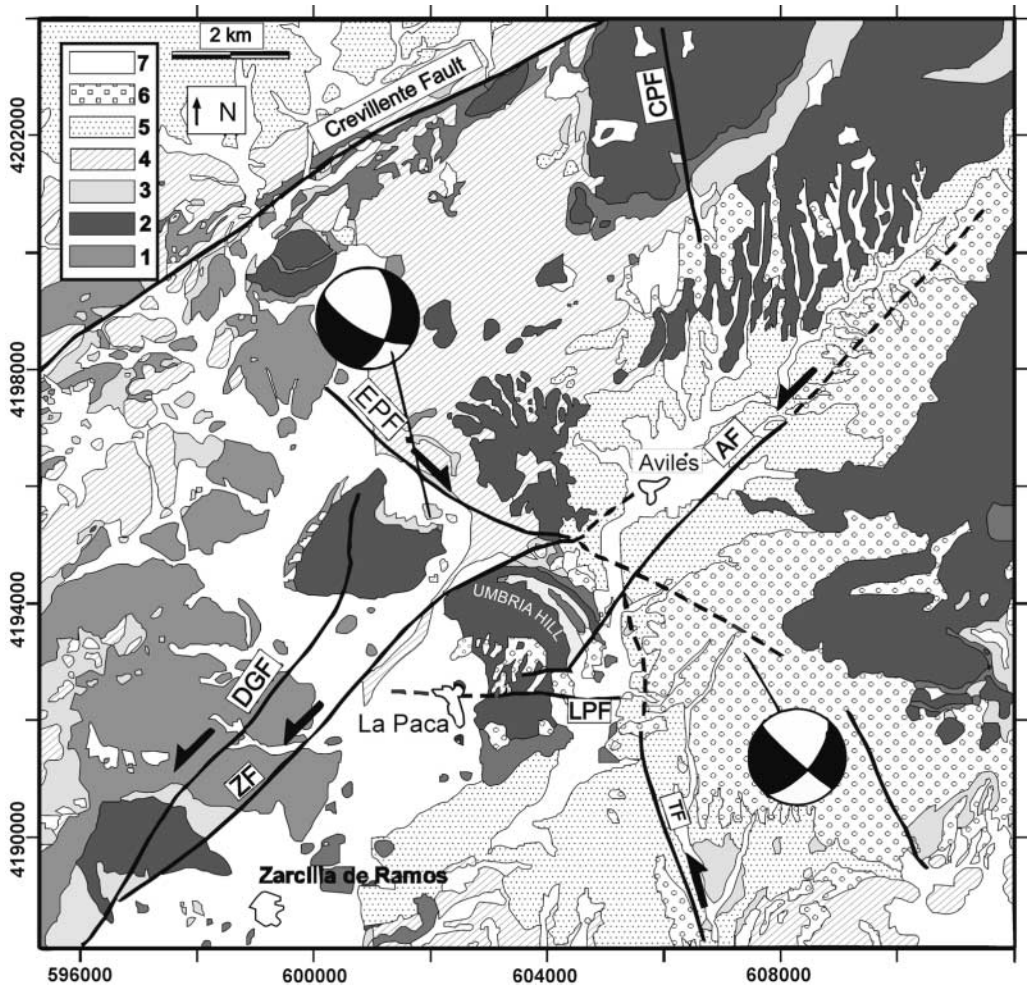

Figure 8. Simplified geological and tectonic map of the epicentral area, showing the main faults and focal mechanisms solutions for the 2002 and 2005 mainshocks. AF, Avilés fault; TF, Terreras fault; ZF, Zarcilla fault; DGF, Don Gonzalo fault; EPF, El Puerto fault; LPF, La Paca fault; CPF, Cerro Pelado fault; 1, Triassic; 2, Jurassic; 3, Cretaceous; 4, Paleogene; 5, Pliocene; 6, Plio-Quaternary; 7, Quaternary.

Table 4
Summary of Local Fault Characteristics

Name	Label in Figure 8	Strike	Estimated Length (km)	Regime
Avilés fault	AF	N40–45	11	Left-lateral strike slip
Terreras fault	TF	N161	13	Left-lateral strike slip
Zarcilla fault	ZF	N48	9–11	Left-lateral strike slip
Don Gonzalo fault	DGF	N45	8	Left-lateral strike slip
El Puerto fault	EPF	N125	6–8	Normal, right-lateral strike slip
La Paca fault	LPF	N90	4.5	Thrust?
Cerro Pelado fault	CPF	N75–80	4.5	Left-lateral strike slip

Coulomb static stress increased more than 0.4 bars after the 2002 event. The two major aftershocks also occurred in areas of increased Coulomb stress. In summary, stress change modeling supports the fact that an earthquake-triggering process is active in the area.

Macroseismic Effects of the La Paca (2005) Earthquake and Ground Motion

Damage Distribution

The 2005 La Paca earthquake caused remarkable damage to traditional and engineered structures, considering its

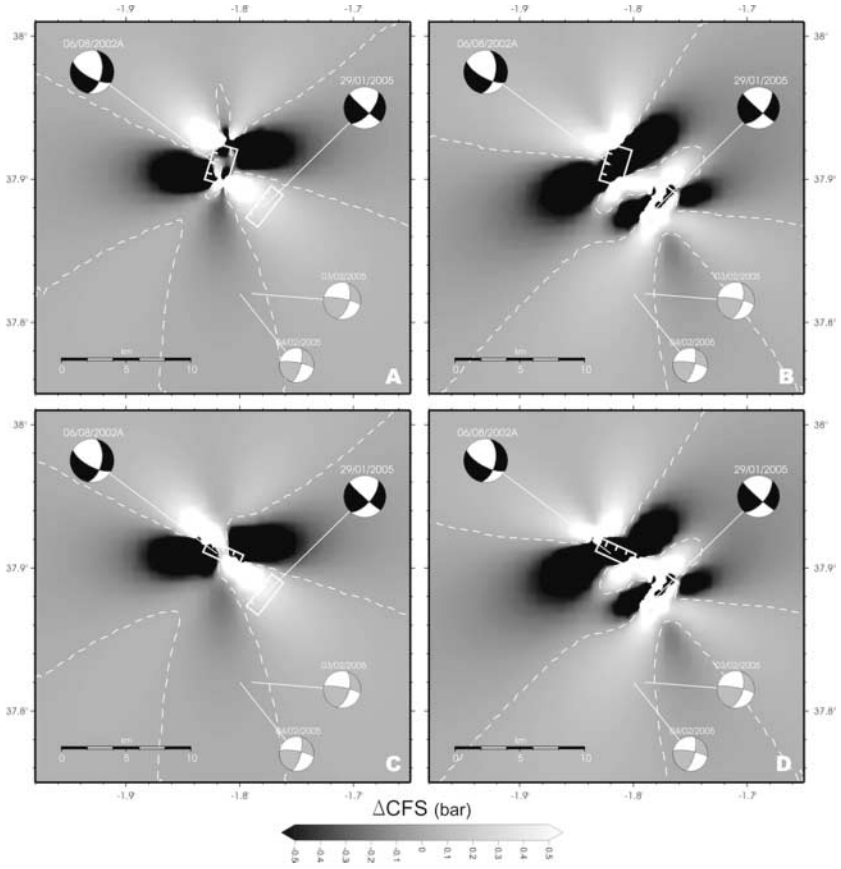

Figure 9. Models of change in static Coulomb failure stress (CFS) generated after the events of 2002 and 2005. Dashed line represents the line of no change. (a) and (b) Changes in CFS produced on planes northeast–southwest (parallel to the fault assumed to be the source of the 2005 earthquake) by the two plane solutions of the 2002 event. (c) and (d) Changes in the CFS produced by the 2002 and 2005 mainshocks on planes optimally oriented under the current tectonic regime. All models are calculated for the hypocentral depth of the 2005 mainshock (3 km).

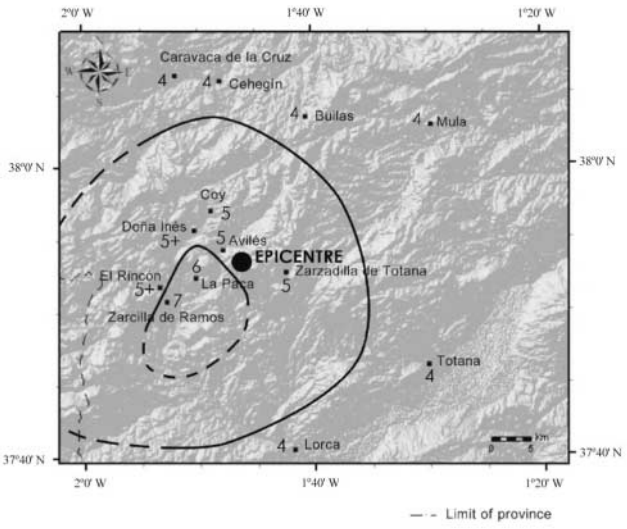

Figure 10. Intensity map (EMS scale) for the La Paca earthquake (29 January 2005).

moderate magnitude of M_w 4.8, and it caused great alarm in local neighborhoods. Intensity distributions show a considerable drift from the epicentral location toward the south-southwest Avilés fault, probably associated with local ground conditions (see next section). An isoseismal map for this event is shown in Figure 10. Maximum EMS intensities of VI and VII were observed at La Paca and Zarcilla de Ramos, respectively, based on macroseismic fieldwork carried out on site. Other locations with shorter epicentral distances, such as the town of Avilés, experienced lighter intensity values (EMS V).

Numerous families were housed provisionally in tents during the first days of the seismic series, while damage assessments were carried out in their homes. Emergency services from the region of Murcia including firemen, Red Cross, and civil defense personnel, supported by architects and psychologists, were deployed to aid some 2000 affected people in the macroseismic area.

As a consequence of the mainshock, many buildings in the affected towns were rendered uninhabitable, most of them in Zarcilla de Ramos. More than 800 damage reports (about 60% of the buildings of La Paca and Zarcilla de Ramos) were claimed. More than 20 houses were initially listed as unsafe and demolished. Most of them were poor-quality traditional structures, evidencing once again the poor performance of unreinforced masonry structure. However, considerable nonstructural damage and slight structural damage was reported to code-compliant reinforced concrete frame buildings, despite only moderate shaking.

No major field effects were observed, although different locations in the epicentral area were still littered with large block falls originating from the 2002 series. Preliminary estimated losses of the earthquake are about 10 million €.

Damage patterns according to building types are presented next.

Damage to Unreinforced Masonry Structures (URM). URM structures form the main building stock of pre-1960s construction in towns and cities across Spain. Masonry is still a significant choice for small-scale, normal technology and economic construction, in general, used for housing in the form of concrete masonry units (CMUs). This type of masonry should be reinforced to be code-compliant (NCSE-94, NCSE-02), but there is little evidence CMUs are actually reinforced in ordinary construction in current practice.

The most significant damage trend observed is the loss of connection between masonry walls due to inertial forces. This type of failure is common in fieldstone construction because true bonds between walls are difficult to achieve due to the nature of the material. Large inertial forces are generated perpendicular to the plane of the walls as the ground shifts during an earthquake, causing them to crack and drift apart from each other. Figure 11a illustrates the deformation and rupture process. Damage of this type is typically grade 2 in buildings of vulnerability A or B. Advanced failure results in out-of-plane wall collapse and is typically grade 3 or 4. Unsupported gable walls are particularly prone to this type of damage. Damage to nonstructural elements such as cornices, eaves, and chimneys was widespread and probably represents the largest risk in moderate earthquakes because this type of damage falls out into crowded streets with light shaking. Some examples of damage in this type of structure are shown in Figure 11b–e.

Damage to Reinforced Concrete Structures (RC). The main damage trends observed in RC buildings was damage to nonstructural elements like walls and infill panels. There was ample evidence of partition walls becoming loaded during the earthquake as shown by widespread shear cracking. Excessive drift and deflection of RC structures is the main cause of this type of damage, resulting in unforeseen loading and participation of partition walls. The combination of rigid partitioning walls and RC frames are always problematic unless the latter are properly stiffened to limit drift and deflection, or the former are strengthened to properly participate as shear walls (Fig. 12a). In any case, the need for improvement in the seismic performance of RC frames with brick infill panels is clear, and this should form the basis for specific and unambiguous attention in further revisions of the Spanish Building Code. Some examples of the damage observed in this type of structure are shown in Figure 12b–d.

Objects and Furniture. In many households furniture was displaced about 10 cm from their original locations and objects fell from shelves, covering the floors of supermarkets with fallen produce. In some households cabinet or refrig-

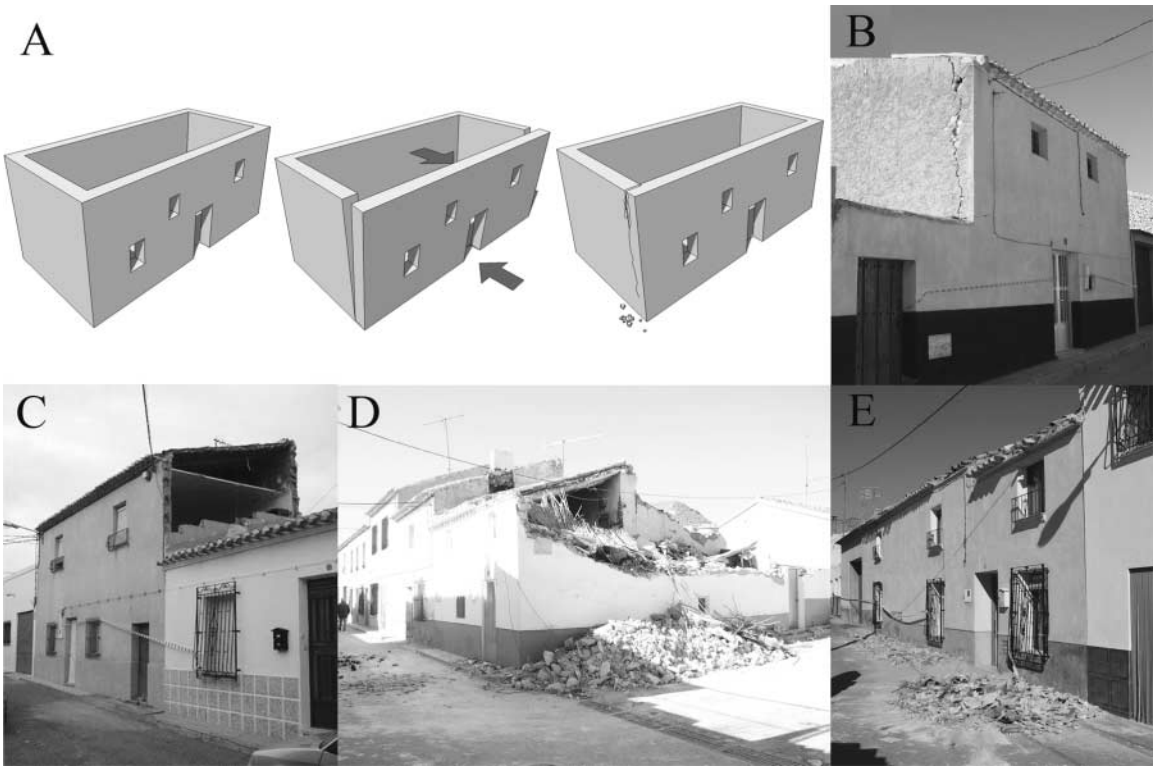

Figure 11. Masonry buildings: (a) Model for out-of-plane wall drift; (b)–(e) Examples of observed damage to these types of buildings.

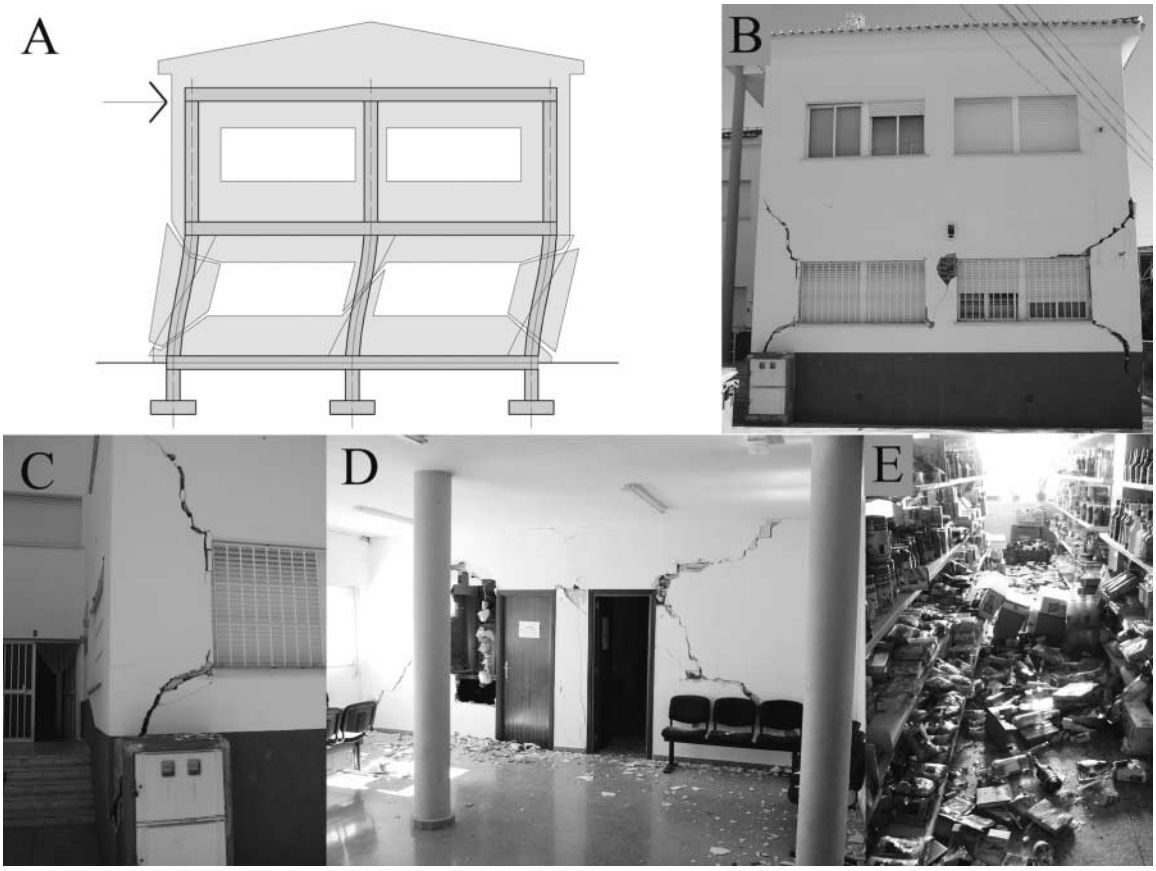

Figure 12. Concrete frame buildings: (a) Deformation process and shear transfer to nonstructural walls through lack of rigidity; (b, (c), and (d) Examples of damage observed in one of these buildings; (e) Objects thrown down from shelves in the same location.

erator doors were flung open and their contents thrown out. Many objects were thrown down from shelves (Fig. 12e), including large objects such as TV sets.

Geotechnical Studies

The aforementioned structural damages of the La Paca earthquake in La Paca and Zarcilla de Ramos seem to depend on not only the magnitude of the earthquake and the distance from the source, but also on local geological conditions that could have resulted in an increase in the intensity of ground motion in both towns. In this regard, we have carried out a detailed study of the geological materials in the epicentral area to determine their possible contribution to local ground amplification.

A general engineering classification of the geological materials based on the existing 1:50,000 scale surface geology map of the area from IGME (Baena Perez, 1972; Kampschuur *et al.,* 1972a) was done to evaluate possible earthquake amplifications for each geological unit. The methods proposed by Borcherdt (1994a, b) and contained on the 2003 National Earthquake Hazards Reduction Program (NEHRP) Provisions (Building Seismic Safety Council, 2003) were adopted for this purpose.

According to the NEHRP classification, the amplification effect in the earthquake area (Table 5) varies from nil (classes A and B), where bedrock is exposed (hard to medium rocks represented by dolomite and limestone and of Jurassic and Cretaceous age), to high (class D) where Plio-Quaternary fluvial sediments are present. Some igneous rocks (class C_1 and C_2) are also found in the area. Because of the similarity and the heterogeneous nature of Quaternary sediments, in the surface geology map, it was not possible to identify soil class E in this area.

The greater part of the soil (which in the geological map corresponds to the Plio-Quaternary fluvial and alluvial fans) in the epicentral area, belongs to either the stiff C_2 silty-sand soils, interspaced with some cemented conglomerates, or to the soft to medium stiff silty-sand soil, corresponding to class D. Zarcilla de Ramos and La Paca are located mainly in this soil class, which exhibits high amplification according to the NEHRP classification. Avilés, on the other hand, with minor damage and nearest to the epicenter, is located in soils of C_2–D classes (high to moderate amplification).

In addition, a detailed evaluation of soil amplification factors was carried out based on the analysis of samples collected on site in the three towns. This was done mainly to confirm the previous surface geology classification. The

Table 5
Categories for Soil Susceptibility to Amplification in the Epicentral Area of the 2005 La Paca Earthquake, Based on Data from the Geological Map

Soil Type	Engineering Classification	Description on the Geological Map	Estimated V_s (m/sec)	Susceptibility to Amplification
Category A	Hard rocks	Jurassic limestone, dolomites and Ophites	>1500	Nil
Category B	Medium strength rocks	Jurassic and Cretaceous interbedded limestones and marly clays	750–1500	Low
Category C_1	Soft rocks and hard soils (very stiff plastic clays)	Kuiper, varied color plastic clays and gypsum	450–750	Moderate
Category C_2	Stiff cohesive soils; interbedded hard cohesionless and cohesive soils.	Tertiary and Plio-Quaternary fluvial and alluvial calcareous cemented conglomerates	350–450	Moderate-high
Category D	Stiff medium soils; small total thickness of soft to medium soils.	Plio-Quaternary fluvial and alluvial loose silty sediments	350–180	High
Category E	Soft soils with total thickness > 10 m.	These soils are not identified very well in the geological map, but occur frequently in the area. A detailed study to identify them is necessary.	<180	Very high

Definitions are based on the soil classification of the 2003 NEHRP Provisions.

results confirm that the soils in the epicentral area that underlay the buildings are mainly unconsolidated and noncemented-detrital, colluvial, and alluvial sediments of continental origin. However, when we compare the results of their geotechnical properties, differences between the soils underlying the three localities (Avilés, La Paca, and Zarcilla de Ramos) are found.

In Zarcilla de Ramos the soils are mainly soft soils 10 m thick or more, consisting of a well to medium graded loose sandy-silt and gravel, interbedded with a semirigid silty clay layer. Plasticity is low and the bulk dry density for these layers also is relatively high compared with the surface soils. The natural water content for the whole sediments is less than their plastic limit, which suggests that the stiffness of the interbedded silty clay layer is the result of an apparent cohesion by suction. During wetting and earthquake shaking, these soils can undergo an important reduction in their consistency, behaving as soft soils. Although the soil at Zarcilla de Ramos was classified as NEHRP type D, results of our geotechnical study show that a NEHRP type E, with a high-amplification effect, is more appropriate.

Soils in La Paca are more homogenous than in Zarcilla and mainly consist of well-sorted or badly graded silty sands. Their thickness ranges approximately from 3 to 5 m. The water content is near to the plastic limit and their bulk dry density is relatively high in comparison with the Zarcilla de Ramos soils. Thus, a NEHRP class D is confirmed for this soil.

Soils in Avilés consist of a superficial (1–2 m) reddish brown silty-clay with some gravels and a thick (more than 30 m) calcareous-cemented Plio-Quaternary conglomerates and marls (very hard and stiff soils), which are more consistent than the soils in the Zarcilla de Ramos and La Paca. A class D–C_2 is thus assigned, in agreement with the first geological classification.

Taking into account the geological and geotechnical data in the selected areas, we propose a geotechnical classification map for the epicentral region, shown in Figure 13. A major change regarding the original classification is introduced in Zarcilla de Ramos, where a class D has been changed to class E (soft clays). In this sense, it can be concluded that the soils underlying the damaged areas, especially in Zarcilla de Ramos, may have played an important role in seismic amplification.

Ground Motion

Several strong-motion stations from the IGN network recorded the 29 January 2005 La Paca earthquake (see Table 6). Most of these stations were located at epicentral distances farther than 20 km and, consequently, the recorded PGA values were relatively low (less than 0.024*g*). The distribution of recorded ground motions is illustrated in Figure 14a. Note the larger amplitude recorded in the stations located in the northeast–southwest direction compared with the ones located to the southeast with respect to the epicenter. A combination of local characteristics at the recording sites and a channeling effect of seismic energy along the northeast–southwest direction, parallel to the main tectonic faults in the area, may explain this observation (Gaspar-Escribano and Benito, 2007).

To estimate the impact of ground motion in the damaged towns of the epicentral areas, we followed the approach of Gaspar-Escribano and Benito (2007) and applied it to Zarcilla de Ramos (R_{ep} = 10 km) and La Paca (R_{ep} = 5 km). The simulation method of Sabetta and Pugliese (1996) is used to reproduce the acceleration time-histories for these towns, taking M_w 4.8 and the soil factors established in the previous geotechnical study (Fig. 14b). Predicted PGA values are about one order of magnitude larger than the recorded PGAs at the stations. At the same time, the empirical ground-motion models of Ambraseys *et al.* (1996), Sabetta and Pugliese (1996), and Berge-Thierry *et al.* (2003) are also used to estimate response spectra at Zarcilla de Ramos and La Paca. The magnitude and distance definitions and specific

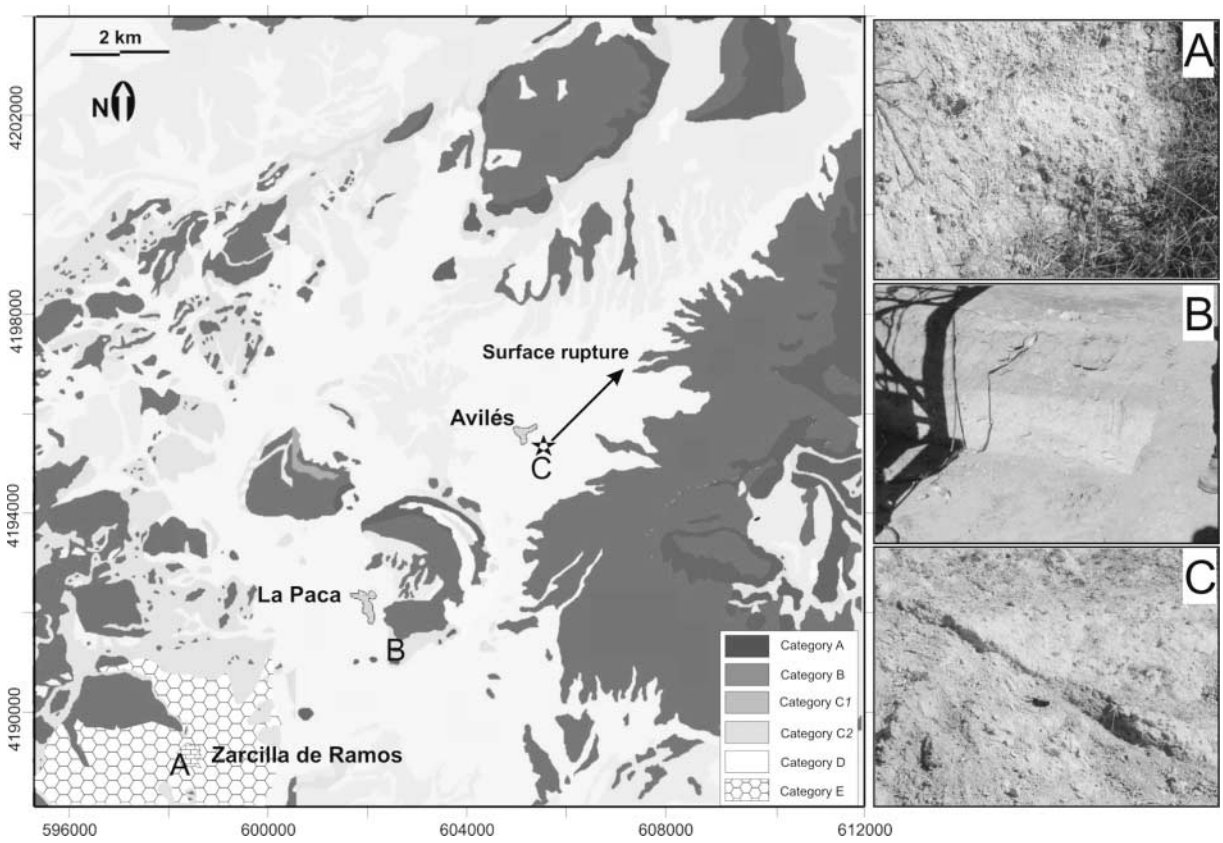

Figure 13. Map of soils in the La Paca earthquake epicentral area, indicating the seismic-amplification susceptibility categories. The pictures show representative soils of the area (see locations on the map).

Table 6
Location of IGN Strong-Motion Stations and Recorded PGA Values of the 29 January 2005 Earthquake

Station	Code	Longitude (° W)	Latitude (° N)	Repic (km)	PGA NS (g)	PGA V (g)	PGA EW (g)
Mula	MUL	1.49	38.04	27	0.024	0.002	0.024
Lorca	LOR	1.70	37.68	28	0.007	0.004	0.006
Alhama de Murcia	AHM	1.43	37.85	32	0.006	0.004	0.003
Vélez Rubio	VLR	2.07	37.65	42	×	0.008	0.011
Murcia	M02	1.13	37.98	56	0.003	0.003	0.003
Jumilla	JUM	1.33	38.48	72	0.006	0.004	0.005
Olula del Río	OLU	2.46	37.35	80	0.002	0.001	0.001
Jaén	JAE	3.79	37.77	179	0.002	0.001	0.002

parameters used for each site, after the necessary adjustments, are listed in Table 7, together with the PGA values estimated using the different methods cited earlier. Average PGA values around 0.1*g* can be derived for both sites.

The empirical and simulated spectra are plotted in Figure 14c, together with the response spectrum derived from the Spanish Building code NCSE-02 for a return period of 475 years. All the estimated spectra for both sites consistently show that maximum spectral accelerations (SA) are reached in intermediate periods (from 0.1 through 0.3 sec), although their amplitudes vary depending on the model used. For the site at La Paca, the NCSE-02 response spectrum exceeds the calculated spectra for periods longer than 0.15 sec. For the site at Zarcilla de Ramos, the NCSE-02 response spectrum exceeds the calculated spectra for the whole-period range. The damage pattern observed in Zarcilla de Ramos, more severe than in La Paca with similar vulnerability of buildings, suggests that the ground motion may have been stronger than the one predicted by simulations and empirical models.

The underestimation of the spectral accelerations may be the result of the soil factor used, which does not reflect

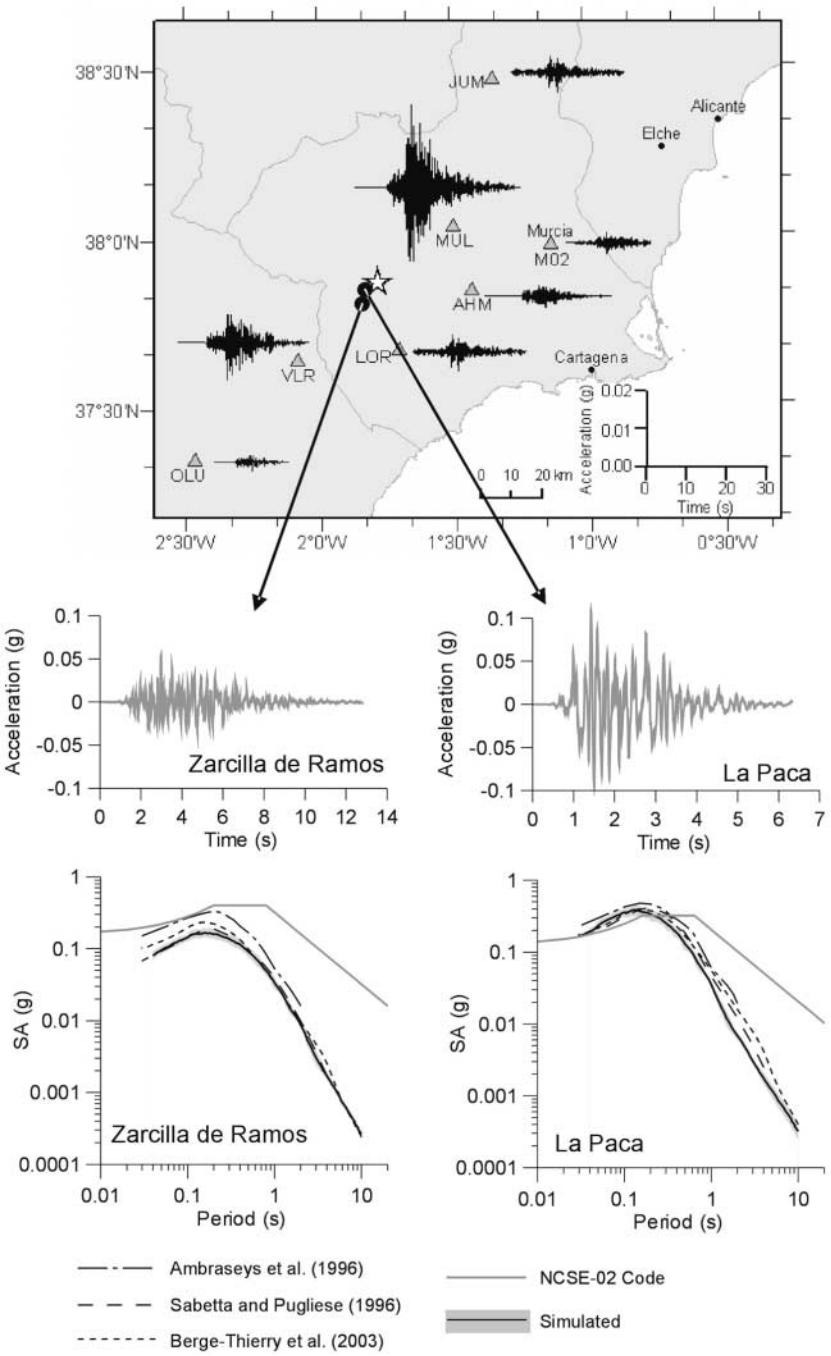

Figure 14. (Top) Geographical distribution of recorded ground motions (north–south components are shown, except at station VLR, where the east–west component is shown). The star indicates the location of the epicenter and the triangles the location of the IGN stations. (Middle) Simulated acceleration time histories using the method of Sabetta and Pugliese (1996) at Zarcilla de Ramos (left) and La Paca (right). (Bottom) NCSE-02 and predicted response spectra at Zarcilla de Ramos (left) and La Paca (right).

accurately the elevated soil amplifications that apparently occurred in Zarcilla de Ramos. This is clear evidence for the need to develop detailed geotechnical studies for providing transfer functions for these soil types. More realistic response spectra would be more in accord with the ground motions experienced, helping to explain the observed damage.

The need to define more accurately local effects in ground motion should be extended to the response spectra included in the Spanish Building Code NCSE-02. This is particularly important for the area of study because earthquakes of larger magnitude than those analyzed are expected. During one of these events, it appears that the NCSE-02 response spectra would be exceeded to an even larger degree than that observed in the present study, questioning the spectra proposed in the code.

Summary and Conclusions

This article presents a complete overview of the 29 January 2005 La Paca earthquake. The earthquake sequence is composed of two subevents of magnitudes M_w 4.8 and 4.2. Moment-tensor inversions show a predominately strike-slip movement with a minor normal component for the main-

Table 7
Parameters Used in the Different Models for Estimating PGA and Spectral Accelerations in the Epicentral Area (Sites La Paca and Zarcilla de Ramos)

Parameters Used in the Different Models		La Paca	Zarcilla de Ramos
Type of distance (km)	Epicentral (R_{ep})	5.0	10.0
	Joyner–Boore (R_{jb})	1.5	5.0
	Hypocentral (R_{hyp})	6.5	11.0
Ground-motion model, soil type considered (and estimated PGA)	Ambraseys *et al.* (1996)	Stiff soil (0.23g)	Soft soil (0.15g)
	Sabetta and Pugliese (1996)	Shallow alluvium (0.11g)	Deep alluvium (0.11g)
	Berge-Thierry *et al.* (2003)	Soil (0.17g)	Soil (0.10g)
	Simulation	Shallow alluvium (0.12g)	Deep alluvium (0.06g)
	NCSE-02	Soil III	Soil IV
Earthquake magnitude	M_w 4.7; M_s 4.7; m_{bLg} 4.7		

PGA values (in g) estimated in both locations, using different empirical ground-motion models and a simulation method, are also indicated.

shock, and a larger normal component for the main aftershock. These results are consistent with a double-rupture event and reveal complex source geometry, with an off-fault origin for the aftershocks.

Several faults with neotectonic activity are identified in the epicentral area. The so-called Avilés fault is the most likely source of the mainshock. A simplified model of fault kinematics in the epicentral area is consistent with a strong compressive deformation and stress concentration around the source area of the 2005 La Paca earthquake. In addition to this stress concentration, the increase of static Coulomb stresses produced after the 2002 southwest Bullas earthquake in an adjacent area may have acted as a triggering mechanism for the 2005 event. This result reveals the significance that triggering interactions may have in southeastern Spain and constitutes an important issue to be considered in future probabilistic seismic-hazard studies.

Based on a broad survey of damage in different locations of the epicentral area, a maximum EMS intensity of VII is assigned to Zarcilla de Ramos. The most significant damage trend observed in URM structures was the loss of connection between masonry walls due to inertial forces. Damage to nonstructural elements was widespread and probably represents the largest risk in moderate earthquakes. The main damage trends observed in RC buildings were damage to nonstructural elements like infill panels, revealing the poor interaction between structural and nonstructural elements in this type of construction. The need for improvement in the seismic performance of RC frames with brick infill panels is evident and should be the focus of further revisions of the Spanish Building Code.

Besides the high vulnerability of buildings, the severity of ground motions in the epicentral area played a significant role on the distribution of damage. Soft soil layers underlying La Paca and Zarcilla de Ramos amplified ground motions to a significant degree. Modeling results show that for short periods predicted spectral accelerations may have exceeded the ground-motion levels of the NCSE-02 code. Therefore, the revision of the soil factors proposed in the code would be useful.

Acknowledgments

The Spanish Instituto Geográfico Nacional (IGN) is acknowledged for providing the strong-motion data used in this work. The focal mechanism analysis was based on high-quality seismic broadband data from Instituto Andaluz de Geofisica, IRIS, and ROA/UCM/Geofon stations, as well as the temporary TEDESE experiment for events in 2002. The authors thank Associate Editor Dr. Lorraine Wolf and two anonymous reviewers for their valuable comments and corrections, which highly improved the quality and comprehensibility of the article. This work has been partly financed by projects CGL2005-04541-C03-01/BTE and CGL2005-07456-C03-03/BTE of the Spanish Ministerio de Educación y Ciencia.

References

Ambraseys, N. N., K. A. Simpson, and J. J. Bommer (1996). Prediction of horizontal response spectra in Europe, *Earthquake Eng. Struct. Dyn.* **25,** 371–400.

Andrieux, J., J.-M. Fontbote, and M. Mattauer (1971). Sur un modele explicatif de l'arc de Gibraltar, *Earth Planet. Sci. Lett.* **12,** 191–198.

Badal, J., E. Samardjieva, and G. Payo (2000). Moment magnitudes for early instrumental Iberian earthquakes, *Bull. Seism. Soc. Am.* **90,** 1161–1173.

Baena Perez, J. (1972). Mapa y memoria explicativa de la Hoja 931 (Zarcilla de Ramos), scale 1:50,000, IGME.

Berge-Thierry, C., F. Cotton, O. Scotti, D.-A. Griot-Pommera, and Y. Fukushima (2003). New empirical response spectral attenuation laws for moderate European earthquakes, *J. Earthquake Eng.* **7,** no. 2, 193–222.

Borcherdt, R. D. (1994a). Estimates of site-dependent response spectra for design (methodology and justification), *Earthquake Spectra* **10,** 617–653.

Borcherdt, R. D. (1994b). Simplified site classes and empirical amplification factors for site-dependent code provisions, in *Proceedings of the NCEER/SEAOC/BSSC Workshop on Site Response during Earthquakes and Seismic Code Provisions, University of Southern California, Los Angeles, November 18–20, 1992*, G. M. Martin (Editor), National Center for Earthquake Research Special Publication NCEER-94-SP01, Buffalo, New York.

Braunmiller, J., U. Kradolfer, M. Baer, and D. Giardini (2002). Regional moment tensor determination in the European-Mediterranean area—initial results, *Tectonophysics* **356,** 5–22.

Buforn, E., and C. Sanz de Galdeano (2001). Focal mechanism of Mula (Murcia, Spain) earthquake of February 2, 1999, *J. Seism.* **5,** 277–280.

Buforn, E., B. Benito, C. Sanz de Galdeano, C. del Fresno, D. Muñoz, and

I. Rodríguez (2005). Study of the damaging earthquake of 1911, 1999 and 2002 in the Murcia (SE Spain) region, *Bull. Seism. Soc. Am.* **95,** 549–567.

Building Seismic Safety Council (BSSC) (2003). *NEHRP Recommended Provisions for Seismic Regulations for New Buildings and Other Structures*. Part 1, *Provisions (FEMA 450)*, Building Seismic Safety Council of the National Institute of Building Sciences, Washington, D.C., 340 pp.

Chinnery, M. A. (1963). The stress changes that accompany strike-slip faulting, *Bull. Seism. Soc. Am.* **53,** 921–932.

European Macroseismic Scale 1998 (EMS-98). *Cahiers du Centre Europ. de Géodyn. et de Séismologie* **15,** 1–99.

Freed, A. M., and J. Lin (2001). Delayed triggering of the 1999 Hector Mine earthquake by viscoelastic stress transfer, *Nature* **411,** 180–183.

Galbis, J. V. (1932). *Catálogo sísmico de la zona comprendidad entre los meridianos 5°E y 20°W de Greenwich y los paralelos 45°N y 25°N*, Tomo I, Instituto Geográfico, Catastral y de Estadística, Madrid, 567–569.

Gaspar-Escribano, J. M., and B. Benito (2007). Ground-motion characterization of low-to-moderate seismicity zones and implications for seismic design: lessons from recent, M_w ~4.8, damaging earthquakes in southeast Spain, *Bull. Seism. Soc. Am.* **97,** no. 2, 531–544.

Geller, R. J., and C. S. Mueller (1980). Four similar earthquakes in Central California, *Geophys. Res. Lett.* **7,** 821–824.

Harris, R. A., R. W. Simpson, and P. A. Reasenberg (1995). Influence of static stress changes on earthquake locations in southern California, *Nature* **375,** 221–224.

Hermes, J. J. (1978). The stratigraphy of the Subbetic and the southern Prebetic of the Velez Rubio-Caravaca area and its bearing on transcurrent faulting in the Betic Cordilleras of southern Spain, *Proc. K. Ned. Akad. Wet.* **81,** 1–54.

Hermes, J. J. (1985). Algunos aspectos de la estructura de la Zona Subbética (Cordilleras Béticas, España Meridional), *Estudios geol.* **41,** 157–176.

Instituto Geográfico National (IGN) (1999). Serie sísmica de Mula (Murcia), Segundo Informe General, Subdirección General de Geodesia y Geofísica, Instituto Geográfico Nacional, Madrid, 35 pp.

Jaume, S. C., and L. R. Sykes (1992). Changes in state of stress on the southern San Andreas fault resulting from the California earthquake sequence of April to June 1992, *Science* **258,** 1325–1328.

Jerez Mir, L., F. Jerez Mir, and G. García-Monzón (1974). Mapa Geológico de España. Scale 1:50,000, no. 912, Mula. Instituto Geológico y Minero de España, 30 pp., 1 fold map.

Jimenez Cisneros, D. (1911). *Bol. Real Soc. Española de Historia Natural* **11,** 210–211.

Kampshuur, W., C. W. Langemberg, J. Baena, F. Velando, G. García-Monzón, J. Paquet, and H. E. Rondeel (1972a). Mapa geológico Nacional a escala 1:50,000. n° 932, Coy. Instituto Geológico y Minero de España 1 fold map Mapa y memoria explicativa de la.

Kampshuur, W., C. W. Langemberg, H. E. Rondeel, J. A. Espejo, A. Crespo, and R. Pignatelli (1972b). Mapa y memoria explicativa de la Hoja 953 (Lorca) del Mapa geológico Nacional a escala 1:50,000, IGME.

King, G. C., R. S. Stein, and J. Lin (1994). Static stress changes and the triggering of earthquakes, *Bull. Seism. Soc. Am.* **84,** 935–953.

Langston, C. A., J. S. Barker, and G. B. Pavlin (1982). Point-source inversion techniques, *Phys. Earth Planet. Interiors* **30,** 228–241.

Mancilla, F., C. J. Ammon, R. B. Herrmann, and J. Morales (2002). Faulting parameters of the 1999 Mula earthquake, southeastern Spain, *Tectonophysics* **354,** 139–155.

Martínez-Díaz, J. J. (1998). Neotectónica y Tectónica Activa del sector centrooccidental de Murcia y Sur de Almería, Cordillera Bética (España), *Ph.D. Thesis*, Universidad Complutense de Madrid, 466 pp.

Martínez-Díaz, J. J., E. Masana, J. L. Hernández-Enrile, and P. Santanach (2001). Evidence for coseismic events of recurrent prehistoric deformation along the Alhama de Murcia fault, southeastern Spain, *Geol. Acta* **36,** no. 3–4, 315–327.

Martínez-Díaz, J. J., A. Rigo, L. Louis, R. Capote, J. L. Hernandez-Henrile, E. Carreño, and M. Tsige (2002). Caracterización geológica y sismotectónica del terremoto de Mula (Febrero 1999, Mb = 4.8) mediante la utilización de datos geológicos, sismológicos y de interferometría de RADAR (INSAR), *Geogaceta* **31,** 157–160.

Martínez Solares, J. M., and J. Mézcua (2002). *Catálogo sísmico de la Península Ibérica (880 a. C.-1900)*, Monografía 18, Instituto Geográfico Nacional, Madrid, 253 pp.

Mézcua, J., and J. M. Martínez Solares (1983). *Sismicidad del área Iberomogrebi*, Instituto Geográfico Nacional, Madrid, Pub. 203, 301 pp.

Norma de la Construcción Sismorresistente Española (NCSE-94) (1994). Real Decreto 2543/1994, de 29 de diciembre, por el que se aprueba la norma de construcción sismorresistente: parte general y edificación, *Boletín Oficial del Estado* **33,** 3935–3980.

Norma de la Construcción Sismorresistente Española (NCSE-02) (2002). Real Decreto 997/2002, de 27 de septiembre, por el que se aprueba la norma de construcción sismorresistente: parte general y edificación (NCSR-02), *Boletín Oficial del Estado* **244,** 35,898–35,967.

Okada, Y. (1992). Internal deformation due to shear and tensile faults in a half space, *Bull. Seism. Soc. Am.* **82,** 1018–1040.

Omori, F. (1884). On the aftershocks of earthquakes, *J. Coll. Sci. Imperial Univ.* **7,** 111–200.

Pollitz, F. F. (2002). Stress triggering of the 1999 Hector Mine earthquake by transient deformation following the 1992 Landers earthquake, *Bull. Seism. Soc. Am.* **92,** 1487–1496.

Pondrelli, S., A. Morelli, G. Ekström, S. Mazza, E. Boschi, and A. M. Dziewonski (2002). European-Mediterranean regional centroid-moment tensors: 1997–2000, *Phys. Earth Planet. Interiors* **130,** 71–101.

Rey Pastor, A. (1936). Sismicidad de las regiones litorales españolas del Mediterráneo. II Región Bética y Subbética, *Geol. Chaines Betique Subbetique* **4,** no. 1, 20–22.

Rey Pastor, A. (1949). *Comarca sísmica de Caravaca y el sismo del 23 de junio de 1948*, Instituto Geográfico y Catastral, Madrid, 21–33 (in Spanish).

Sabetta, F., and A. Pugliese (1996). Estimation of response spectra and simulation of nonstationary earthquake ground motions, *Bull. Seism. Soc. Am.* **86,** no. 2, 337–352.

Sanchez Lozano, R., and A. Marín (1912). Estudio relativo a los terremotos ocurridos en la provincia de Murcia en 1911, *Bol. Inst. Geol.* **12,** 179–214.

Sanchez Navarro-Neumann, M. M. (1911). Los recientes terremotos murcianos, *Rev. Soc. Astr. España* 119–122.

Sanchez Navarro-Neumann, M. M. (1912). Enumeración de los terremotos sentidos en España durante el año 1911, *Bol. Real Soc. Española Hist. Nat.* 512–518.

Sanchez Navarro-Neumann, M. M. (1917). Ensayo sobre la sismicidad del suelo español, *Bol. Real Soc. Española Hist. Nat.* 100–101.

Sanchez Navarro-Neumann, M. M. (1920). Bosquejo sísmico de la Península Ibérica, in *La estación sismológica y el observatorio astronómico de Cartuja*, Granada, 43–45.

Sanz de Galdeano, C. (1983). Los accidentes y fracturas principales de las Cordilleras Béticas, *Estud. Geol.* **39,** 157–165.

Sanz de Galdeano, C. (1990). Geologic evolution of the Betic Cordilleras in the western Mediterranean, Miocene to present, *Tectonophysics*, **172,** 107–119.

Sanz de Galdeano, C., and E. Buforn (2005). From strike-slip to reverse reactivation: The Crevillente fault system and seismicity in the Bullas-Mula area (Betic Cordillera, southeast Spain), *Geol. Acta.* **3,** 241–250.

Stein, R. S. (1999). The role of stress transfer in earthquake recurrence, *Nature* **402,** 605–609.

Stich, D., C. J. Ammon, and J. Morales (2003). Moment tensor solutions for small and moderate earthquakes in the Ibero-Maghreb region, *J. Geophys. Res.* **108,** 2148, doi 10.1029/2002JB002057.

Stich, D., F. Mancilla, D. Baumont, and J. Morales (2005). Source analysis of the Mw 6.3 2004 Al Hoceima earthquake (Morocco) using regional

apparent source time functions, *J. Geophys. Res.* **110,** B06306, doi 10.1029/2004JB003366.

Stich, D., E. Serpelloni, F. Mancilla, and J. Morales (2006). Kinematics of the Iberia-Maghreb plate contact from seismic moment tensors and GPS observations, *Tectonophysics* **426,** 295–317.

Toda, S., and R. S. Stein (2003). Toggling of seismicity by the 1997 Kagoshima earthquake couplet: A demonstration of time-dependent stress transfer, *J. Geophys. Res.* **108,** B12, 2567, doi 10.1029/2003JB002527.

Toda, S., R. S. Stein, P. A. Reasenberg, and J. H. Dieterich (1998). Stress transferred by the Mw = 6.5 Kobe, Japan, shock: Effect on aftershocks and future earthquake probabilities, *J. Geophys. Res.* **103,** 24,543–24,565.

Velando, F., and J. Paquet (1974). Mapa Geológico de España, Scale 1:50,000, no. 911. Cehegín, Instituto Geológico y Minero de España, 28 pp., 1 fold map.

Wells, D. L., and K. J. Coppersmith (1994). New empirical relations among magnitude, rupture length, rupture width, rupture area and surface displacement, *Bull. Seism. Soc. Am.* **85,** 1–16.

Zeng, Y. (2001). Viscoelastic stress-triggering of the 1999 Hector Mine earthquake by the 1992 Landers earthquake, *Geophys. Res. Lett.* **28,** 3007–3010.

ETSI Topografía, Geodesia y Cartografía
Universidad Politécnica de Madrid
28031 Madrid, Spain
(B.B., J.M.G.-E., M.J.G.R., M.E.J.)

Department de Geodinámica, F. CC. Geológicas
Universidad Complutense de Madrid
28003 Madrid, Spain
(R.C., J.J.M.-D., M.T., J.M.I.-A., J.A.A.-G., C.C.)

Architect
Piamonte 18, 4E 28004 Madrid, Spain
(P.M.)

Istituto Nazionale di Geofisica e Vulcanologia
40128 Bologna, Italy
(D.S.)

Laboratorio de Geotecnia (CEDEX)
Alfonso XII, 3 Madrid 28014, Spain
(J.G.-M.)

Manuscript received 28 July 2005.